

RESEARCH ARTICLE

Hydrogel bioink formulation for 3D bioprinting: Sustained delivery of PDGF-BB and VEGF in biomimetic scaffolds for tendon partial rupture repair

Supplementary File

(A) Ink development

	<u>Selection</u>	<u>Considerations</u>
Gelatin	<ul style="list-style-type: none"> Structural similarity to collagen (main component of tendons) Biocompatibility. Supports cell adhesion, proliferation and differentiation Improves the printability thanks to its response to temperature 	<ul style="list-style-type: none"> Stirring can produce a lot of bubbles that can be difficult to remove when the solution is viscous It can be melt at 37 °C overnight without agitation Can be centrifuged at high velocities to remove the bubbles (1800g). Centrifugation of the solution at 37 °C helps to remove the bubbles more easily The viscosity of the resulting solution is temperature-dependent
Hyaluronic acid	<ul style="list-style-type: none"> Lubrication and viscoelasticity. Reduces the friction, facilitating smooth movement and mimicking the natural lubrication found in healthy tendons Water retention. Helps to maintain a hydrated environment Biocompatibility. It is a polysaccharide found in the ECM 	<ul style="list-style-type: none"> High rates of stirring help the dissolution When in a dissolved state, it is transparent. However, when mixed with other materials, it can be challenging to visually determine whether it is fully dissolved or not. Can be centrifuged at high velocities to remove the bubbles (1800g) Using it in high concentration increases considerably the viscosity of the resulting solution but can affect cell morphology
Alginate	<ul style="list-style-type: none"> Gel-forming ability. By using different cations (as Ca²⁺) a gel can be formed. This cross-linking process is interesting for 3D bioprinting Structurally similar to the ECM. This helps with biocompatibility Water retention 	<ul style="list-style-type: none"> Easy to dissolve using mechanical stirring Transparent when it is dissolved Can be centrifuged at high velocities to remove the bubbles (1800g) Using it in high concentration increases considerably the viscosity of the resulting solution but can affect cell morphology
Fibrinogen	<ul style="list-style-type: none"> Gel-forming ability. By using thrombin a gel can be formed. This cross-linking process is interesting for 3D bioprinting Structurally similar to the ECM. This helps with biocompatibility Biodegradability. It enhances the replacement of the scaffold by newly formed tendon 	<ul style="list-style-type: none"> Can not be dissolved by mechanical stirring or vortex Manual stirring can help it dissolve The solvent should have 0.9% NaCl It can be dissolved at 37 °C under a long incubation time (4 hours for high concentrations) High centrifugation velocities can make it precipitate (up to 1200g) Its dissolution produces a lot of bubbles that are easily removable Solvent can not have FBS. Protein-protein interaction makes it precipitate

Figure S1. Summary of the biological materials selected for the development of the new ink. The first column (Selection) lists the reasons and properties of each material to be selected as component for the development of hydrogel-based scaffolds for partial tendon injuries. The second column (Considerations) includes interesting aspects of the materials to establish the methodology to incorporate them in the ink. Abbreviation: ECM, extracellular matrix.

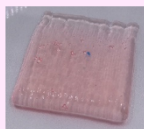

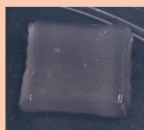

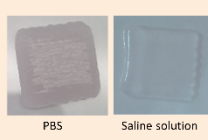
	COMPOSITION			PHOTOS	NOTES
	Biomaterials	Concentration	Solvent		
Formulation 1	Glycerol	100 $\mu\text{L mL}^{-1}$	DMEM		The ink could be easily printed. The obtained scaffolds were difficult to handle. Gelation was achieved enzymatically (fibrinogen-thrombin) and by means of temperature (gelatin).
	Gelatin	35 mg mL^{-1}	DMEM		
	Hyaluronic acid	3 mg mL^{-1}	DMEM		
	Fibrinogen	30 mg mL^{-1}	DMEM		
Formulation 2	Glycerol	120 $\mu\text{L mL}^{-1}$	DMEM		The handling of the obtained scaffold was somewhat easier than that of formulation 1. The other properties did not seem to be very different between the two formulations. Fibrinogen dissolved more easily using DMEM with 0.9% NaCl.
	Gelatin	42 mg mL^{-1}	DMEM		
	Hyaluronic acid	3.6 mg mL^{-1}	DMEM		
	Fibrinogen	36 mg mL^{-1}	DMEM (0.9% NaCl)		
Formulation 3	Glycerol	140 $\mu\text{L mL}^{-1}$	DMEM		The strength of the scaffold appeared very similar to formulation 2 despite having a higher concentration of all components.
	Gelatin	49 mg mL^{-1}	DMEM		
	Hyaluronic acid	4.2 mg mL^{-1}	DMEM		
	Fibrinogen	42 mg mL^{-1}	DMEM (0.9% NaCl)		
Formulation 4	Alginate	10 mg mL^{-1}	DMEM		The change from glycerol to alginate meant the inclusion in the formulation of a second crosslinking method. The obtained scaffolds were much easier to handle and appeared more resistant.
	Gelatin	42 mg mL^{-1}	DMEM		
	Hyaluronic acid	3.6 mg mL^{-1}	DMEM		
	Fibrinogen	36 mg mL^{-1}	DMEM (0.9% NaCl)		
Formulation 5	Alginate	10 mg mL^{-1}	PBS/ Saline solution		There did not appear to be any differences between formulation 4 and formulation 5 in terms of scaffold handling ability.
	Gelatin	42 mg mL^{-1}	PBS/ Saline solution		
	Hyaluronic acid	3.6 mg mL^{-1}	PBS/ Saline solution		
	Fibrinogen	36 mg mL^{-1}	PBS/ Saline solution		

Figure S2. Formulations developed using the selected biological materials. Different concentrations and methodologies to dissolve/disperse and to combine the biomaterials were studied. This development process was dynamic and allowed the ink to be gradually defined. Formulations 1–3 had the same composition, but the concentration of the different components varied. The scaffolds obtained using these three formulations were very similar in appearance and handled in a similar manner. Glycerol was replaced by alginate in the formulation 4 (thus adding a second crosslinking method). Through this change, it was possible to improve the rheological properties of the ink. Although the obtained scaffolds had a similar appearance visually, the incorporation of alginate made it possible to make them more manageable. The effect of using other solvents instead of the culture medium (formulation 5) was also studied. No improvements were observed in the obtained scaffolds. Formulation 4 was selected as the final ink formulation.

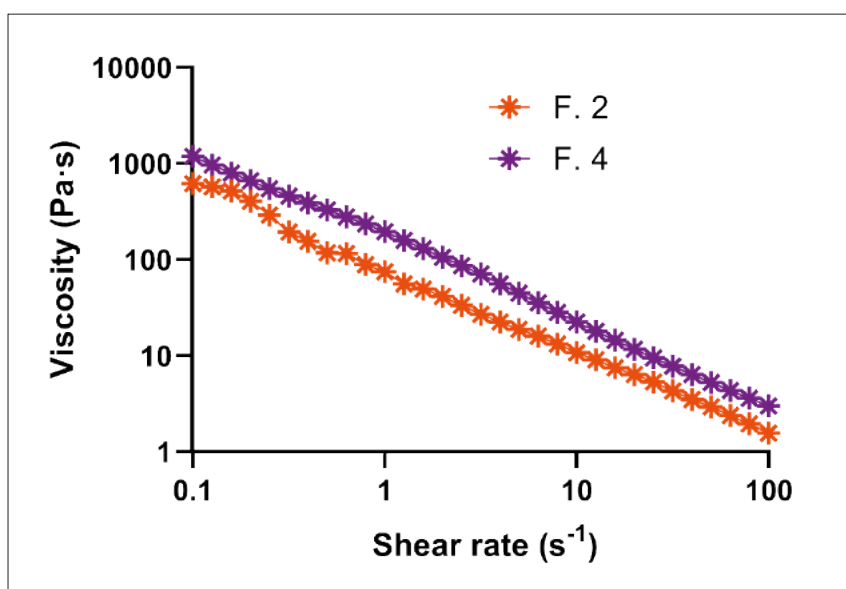


Figure S3. Shear rate sweep assay performed with formulation 2 and formulation 4.

Table S1. Parameter values of the Carreau–Yasuda model for both formulation 2 and formulation 4

Property	Meaning for the 3D printing process	Value for formulation 2	Value for formulation 4
Power-law exponent (n)	It characterizes the shear-thinning behavior. For 3D printing, a shear-thinning material is often desirable as it facilitates extrusion through the nozzle during printing and promotes layer adhesion. $0 < n < 1$: shear thinning $n > 1$: shear thickening $n = 1$: Newtonian fluid	0.14	0.15
Shape parameter (a)	It describes the transition between low and high shear rate behaviors. An appropriate value contributes to a smooth transition in viscosity, avoiding sudden changes during printing.	0.10	0.13
Relaxation time (λ)	It influences how quickly the material responds to changes in shear rate. An optimal λ ensures that the material adapts swiftly to variations in flow conditions during printing.	17.73 s	10.12 s
Zero-rate viscosity (η_0)	It represents the material's viscosity at low shear rates. For 3D printing, a moderate value is often desirable (to ensure that it flows through the printing nozzle but also that it maintains its position once extruded).	1.12×10^{-5} Pa·s	0.18 Pa·s
Infinite-rate viscosity (η_∞)	It represents the viscosity at high shear rates. A lower value is generally preferable for 3D printing, enabling the material to flow easily during the printing process.	1100.62 Pa·s	4039.11 Pa·s
Adjustment of the model (R^2)		0.999833	0.999629

(B) Rheological characterization: parameters

Table S2. Rheological parameters of the developed ink

Property/Parameter ^a	Value	Determined from
Non-Newtonian fluid	Non-linear shear rate/shear stress behavior	Shear rate sweep
Shear thickening	Decrease in viscosity with increasing shear rate	Shear rate sweep
Herschel–Bulkley fluid	Exhibits a non-linear strain rate/shear stress behavior after the yield stress	Shear rate sweep
Zero-rate viscosity	4039.11 Pa·s	Shear rate sweep
Infinite-rate viscosity	0.18 Pa·s	Shear rate sweep
Yield stress (σ_y)	107.48 Pa	Shear rate sweep
Thixotropic behavior	Reversible, time-dependent decrease in viscosity in response to shear rate. 1st cycle: 36.12% recovery after 2 min; 2nd cycle: 24.38% recovery after 2 min	Recovery test
Values in LVER		Strain sweep
G'	323.18 Pa	
G''	114.27 Pa	
G*	342.79 Pa	
Tan δ	0.35	
Linearity limit (γ_L)	67.18%	Strain sweep
Critical strain	345.23% ($G' = G'' = 107.21$ Pa)	Strain sweep
Flow transition index (τ_f/τ_y)	2.28	Oscillation stress
Yield point (τ_y)	232.35 Pa	Stress sweep
Flow point or flow stress (τ_f)	528.83 Pa	Stress sweep
Beginning of gel formation (t_{CR})	3 min 30 s	Time sweep
Gel point (t_{SG})	10 min 10 s	Time sweep
G', G'' stabilization	55 min	Time sweep
Viscoelastic liquid and solid-like gel behavior	G' is higher than G'' for all the frequency range; with increasing frequency both modulus increase	Frequency sweep
Melting temperature (T_m)	23.56°C	Temperature sweep
Gelation temperature (T_g)	28.14°C	Temperature sweep

^a The conditions under which the ink showed these rheological properties are described in the materials and methods section. Abbreviations: G', storage modulus; G'', loss modulus; G*, complex modulus; LVER, linear viscoelastic region.

(C) Printability and printing fidelity

In this work, four parameters were selected to characterize the printability of the developed ink: the formation of filaments, the level of gelation (under-gelation, optimal gelation, and over-gelation), the shape fidelity, and the strand printability. The four tests and the methodology used to determine the values of the mentioned parameters are schematically shown in Figure S4.

The formation of filaments in the 3D extrusion printing process is presented in Figure S4 (panel 1). When the ink is too gelled, the filaments are more curved and have a “clumpy” appearance due to breakage in the printing process of the gel previously created in the syringe (hyper-gelated filament). When the ink has the proper gelation, the filaments do not present discontinuities or gel fragments and are continuous and

uniform (continuous filament). When the ink is under-gelated, no filaments are obtained (no filament-drops). The ink comes out of the syringe needle in the shape of droplets. The second mentioned parameter is the level of gelation (Figure S4, panel 2). The filaments and printed structures can be differentiated in three states: under-gelation, proper gelation, and over-gelation. The third analyzed parameter is the strand printability, and, for that, single filaments are evaluated (Figure S4, panel 3). The diameter of the filaments is measured at different points, and then the media are done. The resulting value is compared with the theoretical diameter of the filament in the CAD design. The parameter is represented as percentage. Finally, the last parameter is the shape fidelity of the printed structures (Figure S4, panel 4). It has different names in literature (*ex.* filament fusion test or deflection test). A structure

with increasing distances between filaments is printed at different printing parameters. The comparison between the obtained areas and the areas in the design

is analyzed. The result of this assay gives information about the filaments as well as the resolution that can be obtained with the ink at the printing conditions.

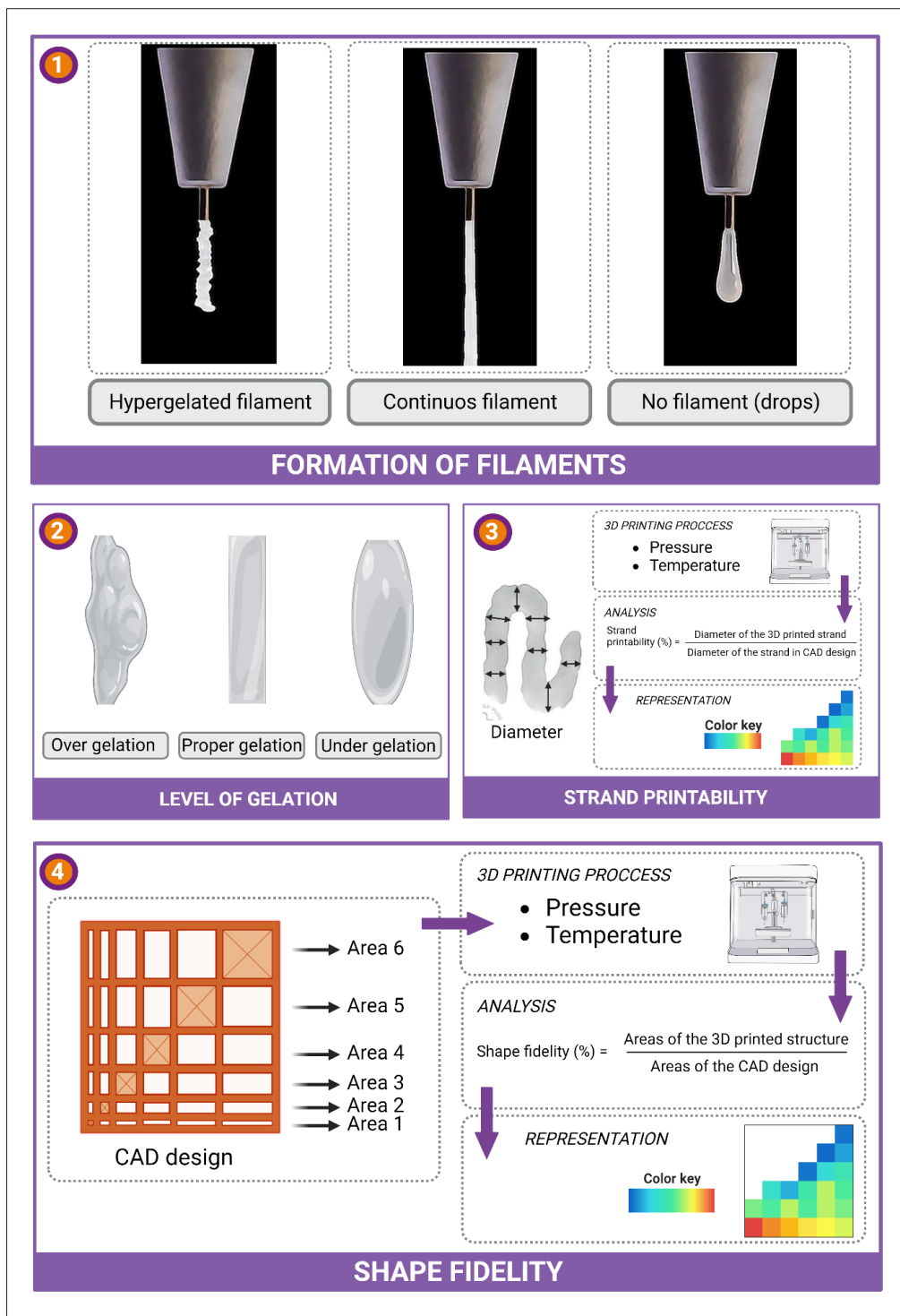


Figure S4. Schematic representation of the printability assays. (1) Analysis of the formation of filaments in the 3D extrusion printing process. (2) Level of gelation observed in the filaments and printed structures. (3) Strand printability. (4) Shape fidelity of the printed structures. Created with Biorender.com

(D) Mechanical properties of the acellular scaffolds and tissue constructs: compressive test

Parameters based on the stress vs. strain curve were analyzed and discussed in the main text. Nevertheless, there are other important parameters that can also be determined from the compressive test. These parameters are the maximum force and the stiffness of the scaffolds and tissue constructs. In this case, instead of using the stress vs. strain curves, the force vs. displacement curves need to be

analyzed (Figure S5). On day 1, the maximum force was observed on the structures: 7.67 N for acellular scaffolds and 6.46 N for tissue constructs. The stiffness value was also higher on day 1: 14.36 N mm⁻¹ for acellular scaffolds and 9.93 N mm⁻¹ for tissue constructs. In the following time points, the structures presented lower mechanical properties. No significant differences were observed between the maximum force of the tissue constructs and the acellular scaffolds. However, statistical differences between tissue constructs and acellular scaffolds were observed in the case of stiffness.

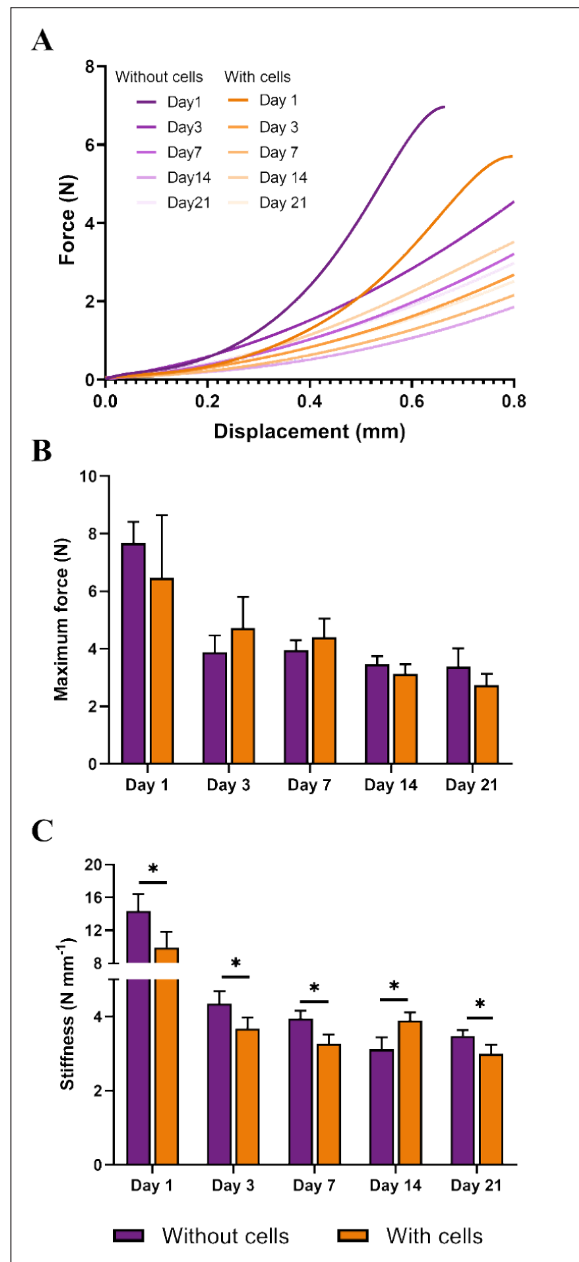


Figure S5. Mechanical characterization of the acellular scaffolds (purple) and tissue constructs (orange). This characterization was performed with a compression test. Results are represented as mean ± SD (n = 4). *p < 0.05.

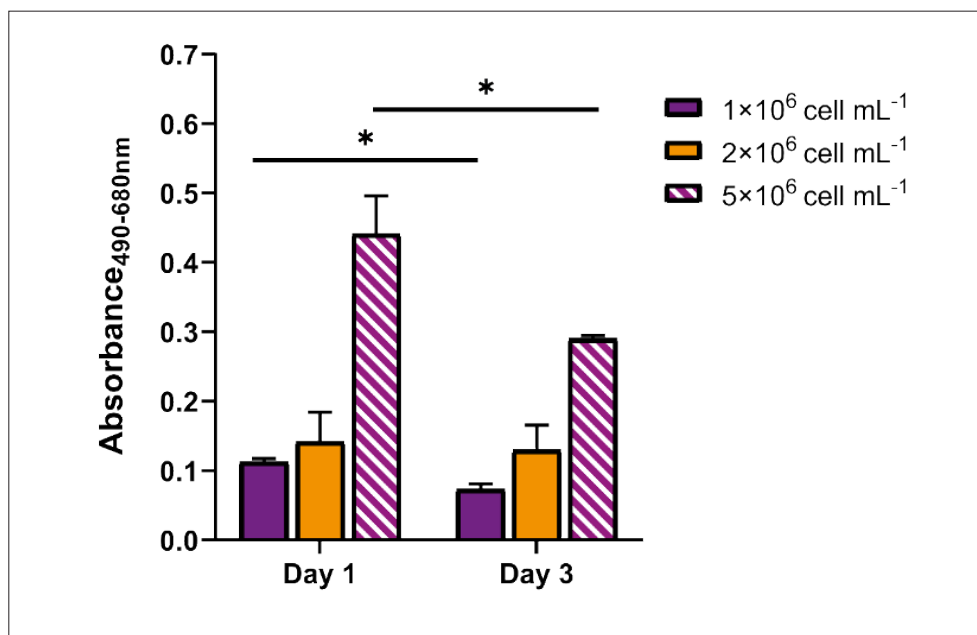
(E) Printing effect on cells (stress)

Figure S6. Lactate dehydrogenase assay. Results are represented as mean \pm SD (n = 3). Statistical differences between days are shown. *p < 0.05.

(F) Correlation between the expressions of tendon-related genes

As mentioned in the main text, the studied genes include scleraxis BHLH transcription factor (*Scx*), tenascin C (*Tnc*), collagen type I alpha 1 chain (*Col1a1*), collagen type III alpha 1 chain (*Col3a1*), Fos proto-oncogene (*c-Fos*), and fibronectin 1 (*Fn1*). Although it was not the main focus of this study, analyzing the correlation between the expressions of different genes is a fundamental aspect of molecular biology and genetics research. Spearman statistics were used to analyze the obtained results (Table S2). The analysis revealed that several of the studied genes showed direct correlation in their expression levels (Figure S7): *Col1a1* with *Fn1*, *Tnc* with *c-Fos*, *c-Fos* and *Tnc* with *Col3a1*, and *Scx* with *Col1a1*. Despite not being statistically significant, there also seems to be a certain direct correlation between *Scx* and *Fn1*. It becomes apparent that there are two clusters of genes with related expressions. In the first cluster, the correlation between *Col1a1* and *Fn1* may be related to the participation of fibronectins in the regulation of type I collagen deposition. Both are molecules of the ECM, thus justifying a similar expression profile. Furthermore, the expression of both genes could be positively regulated by the expression of the *Scx* gene, as described in the literature.^{1,2} In the second cluster, the relationship between *Tnc* and *c-Fos* may be due to

the fact that the expression of both genes increases in response to mechanical stimuli (in this case, it could be due to the compression they suffer within the scaffold).³ No information has been found in the literature to offer an explanation on why the expression of *c-Fos* and *Col3a1* are related.

In the context of the correlation between *Tnc* and *Col3a1*, prior studies in the literature have reported that incubating vascular smooth muscle cells⁴ and human dermal fibroblasts⁵ with Tenascin-C (TNC), a glycoprotein, resulted in the upregulation of *Col3a1* expression. Therefore, in the case of tenocytes embedded in the hydrogel, there could be an upregulation of the expression of type III collagen caused by an increase in the expression of *Tnc*.

References

1. Yoshimoto Y, Takimoto A, Watanabe H, Hiraki Y, Kondoh G, Shukunami C. Scleraxis is required for maturation of tissue domains for proper integration of the musculoskeletal system. *Sci. Rep.* 2017;7:45010. doi: 10.1038/srep45010
2. Bagchi RA, Roche P, Aroutiounova N, et al. The transcription factor scleraxis is a critical regulator of cardiac fibroblast phenotype. *BMC Biol.* 2016;14:21. doi: 10.1186/s12915-016-0243-8

3. Miescher I, Wolint P, Opelz C, et al. Impact of high-molecular-weight hyaluronic acid on gene expression in rabbit Achilles tenocytes *in vitro*. *Int J Mol Sci*. 2022;23(14):7926. doi: 10.3390/ijms23147926
4. Nagel F, Schaefer AK, Gonçalves IF, et al. The expression and role of tenascin C in abdominal aortic aneurysm formation and progression. *Interact. Cardiovasc Thorac Surg*. 2022;34(5):841-848. doi: 10.1093/icvts/ivac018
5. Katoh D, Kozuka Y, Noro A, Ogawa T, Imanaka-Yoshida K, Yoshida T. Tenascin-C induces phenotypic changes in fibroblasts to myofibroblasts with high contractility through the integrin $\alpha\beta1$ /transforming growth factor β /SMAD signaling axis in human breast cancer. *Am J Pathol*. 2020;190(10):2123-2135. doi: 10.1016/j.ajpath.2020.06.008

Table S2. Values of the Spearman correlation coefficient for the analyzed tendon-related genes

	<i>Scx</i>	<i>c-Fos</i>	<i>Tnc</i>	<i>Col1a1</i>	<i>Col3a1</i>	<i>Fn1</i>
<i>Scx</i>	-	-0.286	-0.024	0.738	-0.071	0.69
<i>c-Fos</i>	-	-	0.621	0.095	0.721	0.048
<i>Tnc</i>	-	-	-	0.429	0.700	0.476
<i>Col1a1</i>	-	-	-	-	0.333	0.976
<i>Col3a1</i>	-	-	-	-	-	0.286
<i>Fn1</i>	-	-	-	-	-	-

Abbreviations: *Scx*, scleraxis BHLH transcription factor; *c-Fos*, Fos proto-oncogene; *Tnc*, tenascin C; *Col1a1*, collagen type I alpha 1 chain; *Col3a1*, collagen type III alpha 1 chain; *Fn1*, fibronectin 1.

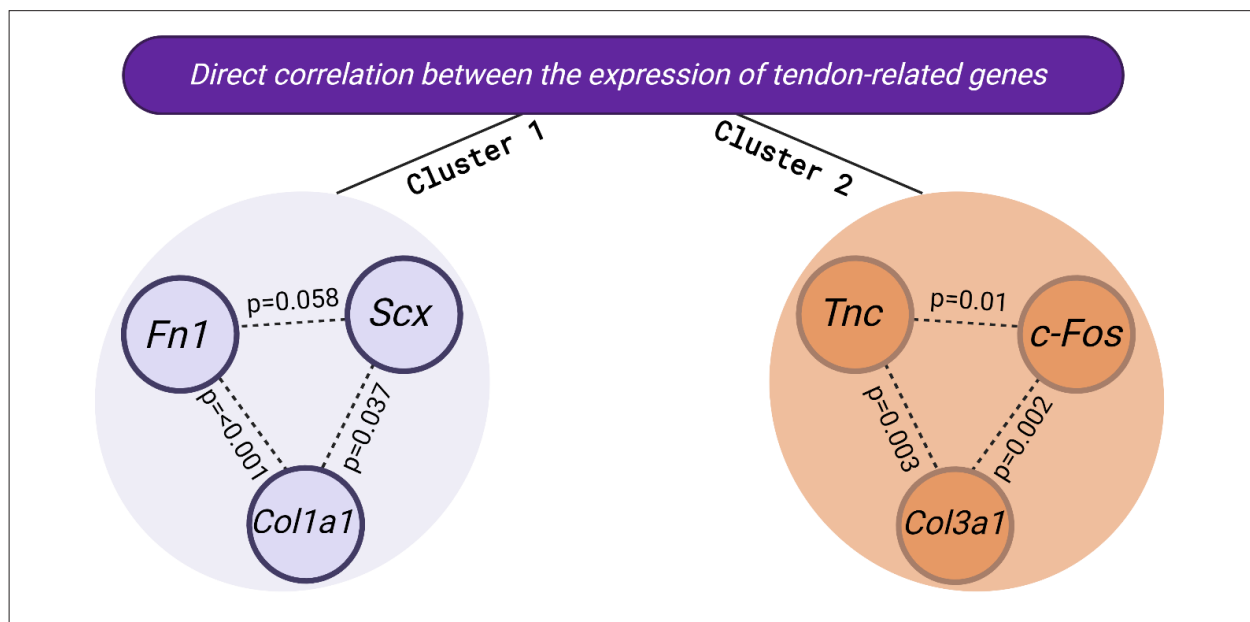


Figure S7. Direct correlation between the expressions of the analyzed tendon-related genes. Spearman statistics were used to analyze the relationship. The *p*-value of the analysis is determined for each pair of genes that showed a statistically significant correlation. Created with Biorender.com. Abbreviations: *Scx*, scleraxis BHLH transcription factor; *c-Fos*, Fos proto-oncogene; *Tnc*, tenascin C; *Col1a1*, collagen type I alpha 1 chain; *Col3a1*, collagen type III alpha 1 chain; *Fn1*, fibronectin 1.